

# Growth and physical properties of single crystalline MgB<sub>2</sub>

C. U. Jung<sup>\*</sup>, Jae-Hyuk Choi<sup>\*</sup>, P. Chowdhury<sup>\*</sup>, Kijoong H. P. Kim<sup>\*</sup>, Min-Seok Park<sup>\*</sup>, Heon-Jung Kim<sup>\*</sup>, J. Y. Kim<sup>\*</sup>, Zhonglian Du<sup>\*</sup>, Mun-Seog Kim<sup>\*</sup>, W. N. Kang<sup>\*</sup>, Sung-Ik Lee<sup>\*</sup>, Gun Yong Sung<sup>†</sup> & Jeong Yong Lee<sup>§</sup>

<sup>\*</sup>National Creative Research Initiative Center for Superconductivity and Department of Physics, Pohang University of Science and Technology, Pohang 790-784, Republic of Korea

<sup>†</sup>Telecommunications Basic Research Laboratory, Electronics and Telecommunications Research Institute, Taejon 305-350, Republic of Korea

<sup>§</sup>Department of Material Science and Engineering, Korea Advanced Institute of Science and Technology, Taejon 305-701, Republic of Korea

We report on the growth of high-quality MgB<sub>2</sub> single crystals. With a hexagonal plate shape the crystal showed shiny surfaces with a length up to about 60  $\mu\text{m}$  and a thickness of 2 - 5  $\mu\text{m}$ . High-resolution transmission electron microscope image indicates hexagonal structure with an *a*-axis lattice constant of 3.09  $\text{\AA}$ . A very sharp superconducting transition at 38 K with a resistive transition width of 0.3 K, and very weak pinning behaviors were observed. Both superconducting parameter such as upper critical field and normal state property such as magnetoresistance showed quite a large anisotropy.

\*To whom correspondence should be addressed. E-mail: silee@postech.ac.kr

The recent discovery of the binary metallic MgB<sub>2</sub> with a superconducting transition temperature of 39 K (ref. 1) has attracted great scientific<sup>2-12</sup> and applicatory interests<sup>13-15</sup>. Although quite a few scientifically important issues have been refined using polycrystalline samples<sup>2-6</sup>, many physical quantities still remained to be clearly verified for the single crystals. Thus, the growth of single-crystal specimen is an urgent subject.

To grow the single crystals, we used a solid-liquid reaction method. A Mg rich precursor was inserted into a Nb tube and sealed in an inert gas atmosphere. Then, we put the Nb tube inside a quartz tube, which was sealed in vacuum. The quartz tube was heated for one hour at 1050 °C, then very slowly cooled to 700 °C for five to fifteen days, and quenched to room temperature. The crystal images were observed using a polarizing optical microscope and using a field-emission scanning electron microscope (SEM). Structural analyses were carried out by the high-resolution

tunneling electron microscopy (HRTEM). The dc magnetic properties were measured with a superconducting quantum interference device magnetometer. Resistivity measurements were also performed by standard dc 4-probe method.

Figure 1 shows the SEM images for various shapes of the MgB<sub>2</sub> single crystals prepared under different synthesis condition, mostly different cooling rates. For the five-day cooling runs, all crystals were found to have a hexagonal plate form with typical edge angles of 120 degrees and with very shiny surfaces. On average, the crystal size was about 20  $\mu\text{m}$  in diagonal length and 2 - 3  $\mu\text{m}$  in thickness, with the largest diagonal length being about 60  $\mu\text{m}$ . Fig. 1(a) shows a typical SEM image for a plate shape crystal.

For the fifteen-day cooling runs, crystals of ball shape and pillar shape were found; in the latter cases, the height was larger than the length of the hexagonal plane, as shown in Fig. 1(b). The diameter of the largest ball-shaped crystal was about 60  $\mu\text{m}$ . These crystals also had clear edge angles of 120 degrees. To measure the temperature and field dependencies of the in-plane resistivity, we used a standard photolithography technique to make four Au electrical leads (bright area) on the top surface of the plate-shaped crystal, as shown in Fig. 1(c).

To confirm the structure of the MgB<sub>2</sub> phase, we took a plane-view HRTEM image of a MgB<sub>2</sub> crystal, which is shown in Fig. 2. In this high-resolution image, the *a*-axis lattice parameter was observed to be  $3.09 \pm 0.06 \text{\AA}$ , which was consistent with the value of polycrystalline samples determined from X-ray powder diffractometry<sup>1</sup>. Figure 2(b) shows the electron diffraction pattern for a selected area with a beam direction of [001] in the hexagonal structure. This result clearly indicates the hexagonal structure of MgB<sub>2</sub>.

Figure 3(a) shows the resistance as a function of temperature from 5 to 300 K. A superconducting transition appeared near 38 K, and the transition width was 0.3 K, based on the 10 to 90% drop of the resistance curve at zero field. The approximate resistivity values at 40 K and 300 K were 1.5 and 7.4  $\mu\Omega\text{-cm}$ , respectively, resulting in a residual resistivity ratio (RRR) of about 5. The reported RRR value of MgB<sub>2</sub> polycrystalline wire was about 25 (refs. 2, 3) whereas those of high-quality *c*-axis oriented thin films were between 2 and 5 (refs. 7, 8). The solid line in Fig. 3 is a fitting curve obtained using the Bloch-Gruneisen formula<sup>16</sup> at the normal state and gives a Debye temperature of  $\theta_D \sim 880 \text{ K}$ , which is consistent with previous reports on the specific heat measurements<sup>4,9</sup>. This suggests that importance of the electron-electron interaction is rather small and that the resistance is dominated by the electron-phonon interaction.

The two insets of Fig. 3(a) show the field dependencies of the in-plane resistance, for fields applied perpendicular to the current path. The value of magnetoresistance at 5 T was found to depend strongly on the direction of the field with respect to the crystal axis. For fields parallel to *ab*-plane ( $H^{\parallel ab}$ ) and to *c*-axis ( $H^{\parallel c}$ ), the magnetoresistance at 40 K were about 21% and 0.5%, respectively.

The simple linear extrapolation of  $H_{c2}^2$  to  $T = 0$  from two data at 0 and 5 Tesla, would give  $H_{c2}^{\parallel ab}(0) = 15.8 \text{ T}$  and

$H_{c2}^{\parallel c}(0) = 9.0$  T, thus the ratio of  $H_{c2}^{\parallel ab}(0) / H_{c2}^{\parallel c}(0) = 1.75 \pm 0.15$ . To determine the temperature dependence of  $H_{c2}$ , we measured the resistance at several field up to 5T. From these curves, we got  $H_{c2}(T)$  as shown in Fig. 3(b), where the 10% drop of resistance was adopted to determine  $H_{c2}$ . We found that the temperature dependence of the upper critical field for field along the c-axis ( $H_{c2}^{\parallel c}$ ) had a large upward curvature, while that for field along the  $ab$ -plane ( $H_{c2}^{\parallel ab}$ ) was nearly linear in the measured temperature and field regions. The ratio of the upper critical field was as high as 3 for  $T \sim 30$  K.

To confirm the bulk properties of the superconductivity, we measured the low-field magnetization curve  $M(T)$  and the magnetic hysteresis curve  $M(H)$ . Since the volume of one crystal is rather small, we fixed about two hundred single crystals on a Si substrate with their  $c$ -axes aligned perpendicular to the substrate surface. Figure 4(a) shows the  $M(T)$  curves measured at 20 Oe in the zero-field-cooling (ZFC) and the field-cooling (FC) modes. The  $T_c$  onset was observed to be  $\sim 38$  K, which is consistent with the value obtained from the resistance measurement. The overall shape was not much different for these two orientations. The different values of magnetic moment for the different field directions gives a demagnetization factor  $D = 0.6$ , which is consistent with the calculated value considering the shape of the crystals.

Figure 4(b) shows the  $M(H)$  curves at 5 K. The  $M(H)$  data shows a negligible paramagnetic background. The difference of  $M(H)$  for increasing and decreasing  $H$  is small, implying the weak pinning nature, which supports that these crystals are very clean. This weak pinning behavior is consistent with a small difference between the magnetizations measured at ZFC and FC conditions, as shown in Fig. 4(a). The different slope of  $M(H)$  at starting low field regions ( $H < 300$  Oe) for different field directions are due to the difference of demagnetization factors.

## REFERENCES AND NOTES

1. J. Nagamatsu, N. Nakagawa, T. Muranaka, Y. Zenitani, J. Akimitsu, *Nature* **410**, 63 (2001).
2. D. K. Finnemore, J. E. Ostenson, S. L. Bud'ko, G. Lapertot, P. C. Canfield, *Phys. Rev. Lett.* **86**, 2420 (2001).
3. P. C. Canfield *et al.*, *Phys. Rev. Lett.* **86**, 2423 (2001).
4. S. L. Bud'ko *et al.*, *Phys. Rev. Lett.* **86**, 1877 (2001).
5. C. -T. Chen *et al.*, Preprint cond-mat/0104285 at <http://xxx.lanl.gov> (2001).
6. H. Kotegawa, K. Ishida, Y. Kitaoka, T. Muranaka, J. Akimitsu, Preprint cond-mat/0102334 at <http://xxx.lanl.gov> (2001).
7. C. B. Eom *et al.*, Preprint cond-mat/0103425 at <http://xxx.lanl.gov> (2001).
8. W. N. Kang, H.-J. Kim, E.-M. Choi, C. U. Jung, S.-I. Lee, *Science* **292**, 1523 (2001).
9. Ch. Walti, *et al.*, Preprint cond-mat/0102522 at <http://xxx.lanl.gov> (2001).
10. C. U. Jung *et al.*, *Physica C* **353**, 162 (2001).
11. Mun-Seog Kim *et al.*, *Phys. Rev. B* (in press), Preprint cond-mat/0102338 at <http://xxx.lanl.gov> (2001).
12. W. N. Kang *et al.*, *Appl. Phys. Lett.* (in press) Preprint cond-mat/0102313 at <http://xxx.lanl.gov> (2001).
13. Y. Bugoslavsky, G. K. Perkins, X. Qi, L. F. Cohen, A. D. Caplin, *Nature* **410**, 563 (2001).
14. D. C. Labalestier *et al.*, *Nature* **410**, 186 (2001).
15. C. U. Jung *et al.*, *Appl. Phys. Lett.* (in press), Preprint cond-mat/0102383 at <http://xxx.lanl.gov> (2001).
16. Charles P. Poole, Jr. *Handbook of Superconductivity*, 31-32 (Academic Press, Florida, 2000).

**ACKNOWLEDGEMENTS.** This work is supported by the Ministry of Science and Technology of Korea through the Creative Research Initiative Program. This work was partially supported by the National Research Laboratory Program through the Korea Institute of Science and Technology Evaluation and Planning.

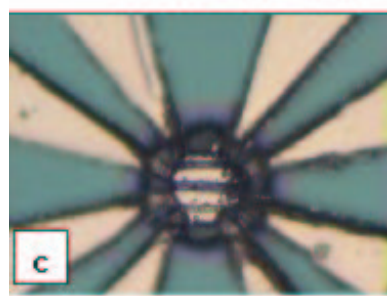
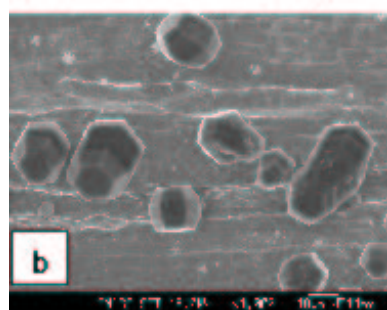
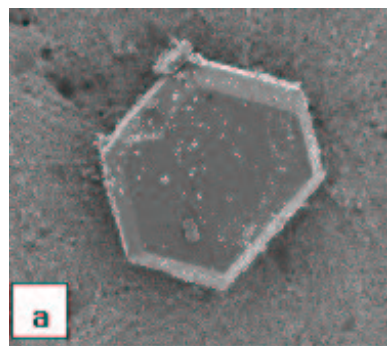
## FIGURE CAPTIONS

Figure 1. SEM and optical microscope images of the  $MgB_2$  single crystals. (a) hexagonal thin plate with a size of about 20  $\mu m$ , (b) ball shaped crystals and pillar shaped crystals, and (c) 4-probe contact leads made on a single crystal by using a photolithography technique to measure the resistance.

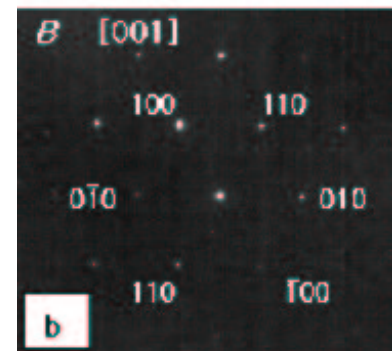
Figure 2. (a) HRTEM image of a  $MgB_2$  single crystal and (b) Selected area diffraction pattern with a beam direction of [001] in the hexagonal structure.

Figure 3. (a) Resistance of a  $MgB_2$  single crystal as a function of temperature for magnetic fields of 0 and 5 T. The residual resistivity ratio is about 5, and the resistivity at 40 K was  $\sim 1.5 \mu\Omega\text{-cm}$ . The insets show the resistance for fields perpendicular and parallel to the crystal. (b) Upper critical field determined from the 10 % drop of resistance for several fields below  $H = 5$  T.

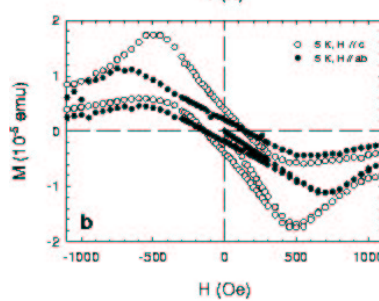
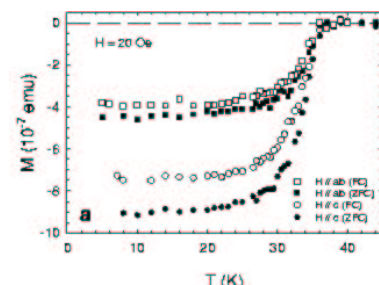
Figure 4. (a) Low-field  $M(T)$  curves of  $MgB_2$  single crystals measured at 20 Oe for fields parallel and perpendicular to the  $c$ -axis. (b)  $M(H)$  hysteresis curves at 5 K.



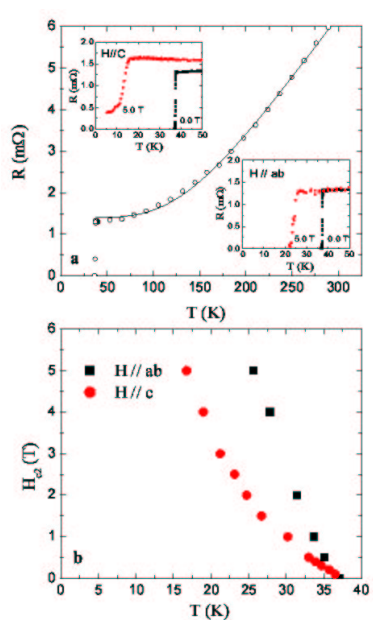
Jung\_Fig1



Jung\_Fig2



Jung\_fig4



Jung\_fig3